

Presenilin influences glycogen synthase kinase-3 β (GSK-3 β) for kinesin-1 and dynein function during axonal transport

Kunsang Dolma, Gary J. Iacobucci[†], Kan Hong Zheng[†], Jayasha Shandilya, Eneda Toska, Joseph A. White II, Elizabeth Spina and Shermali Gunawardena*

Department of Biological Sciences, The State University of New York at Buffalo, Buffalo, NY 14260, USA

Received May 31, 2013; Revised September 2, 2013; Accepted October 3, 2013

Within axons, molecular motors transport essential components required for neuronal growth and viability. Although many levels of control and regulation must exist for proper anterograde and retrograde transport of vital proteins, little is known about these mechanisms. We previously showed that presenilin (PS), a gene involved in Alzheimer's disease (AD), influences kinesin-1 and dynein function *in vivo*. Here, we show that these PS-mediated effects on motor protein function are via a pathway that involves glycogen synthase kinase-3 β (GSK-3 β). PS genetically interacts with GSK-3 β in an activity-dependent manner. Excess of active GSK-3 β perturbed axonal transport by causing axonal blockages, which were enhanced by reduction of kinesin-1 or dynein. These GSK-3 β -mediated axonal defects do not appear to be caused by disruptions or alterations in microtubules (MTs). Excess of non-functional GSK-3 β did not affect axonal transport. Strikingly, GSK-3 β -activity-dependent axonal transport defects were enhanced by reduction of PS. Collectively, our findings suggest that PS and GSK-3 β are required for normal motor protein function. Our observations propose a model, in which PS likely plays a role in regulating GSK-3 β activity during transport. These findings have important implications for our understanding of the complex regulatory machinery that must exist *in vivo* and how this system is coordinated during the motility of vesicles within axons.

INTRODUCTION

Glycogen synthase kinase-3 (GSK-3) is an ubiquitously expressed serine/threonine kinase that is found abundantly in the brain (1,2). The activity of GSK3 controls multiple neurodevelopmental processes, including neurogenesis, neuronal migration, neuronal polarization and axon growth and guidance (3). GSK-3 β activity is highly regulated by phosphorylation (4): phosphorylation of GSK-3 β at Ser9 results in the generation of an intra-molecular pseudo-substrate, which inactivates the enzymatic activity of GSK-3 β (5), while phosphorylation at Tyr216 enhances GSK-3 β activity (4,6). Although phosphorylation is the most common form of regulation, recent work has shown that protein complex formation and intracellular localization also play important regulatory roles in the activity of GSK-3 β (7). Interestingly, changes in GSK-3 activity are associated with many psychiatric and neurodegenerative diseases,

such as Alzheimer's disease (AD), schizophrenia and autism spectrum disorders (4).

An intriguing GSK-3 β -binding protein is presenilin (PS), a key gene involved in AD. Although several reports indicate that GSK-3 β binds to PS (8–10), the functional role this interaction plays is unclear. One study reported a three times increase in the amount of GSK-3 β bound to mutant PS compared with wild-type (WT) PS (9), while another reported that mutant PS bound less GSK-3 β than WT PS (10). Other work demonstrated that mutations of PS decreased its affinity for GSK-3 β relative to WT PS (8). Despite these discrepancies, these studies postulate that GSK-3 β and PS have an important functional relationship, although the significance of this relationship and its affect on disease are unknown.

Two recent studies demonstrated that endogenous PS or GSK-3 β could regulate the bidirectional transport of APP vesicles within axons (11,12). Reduction of PS or GSK-3 β increased

*To whom correspondence should be addressed: The State University of New York at Buffalo, 109 Cooke Hall, North/Amherst Campus, Buffalo, NY 14260, USA. Tel: +1 7166454915; Fax: +1 7166452975; Email: sg99@buffalo.edu

[†]These authors contributed equally to this work.

both the anterograde and retrograde velocities of APP vesicles in *Drosophila* axons, suggesting that PS and GSK-3 β together may directly influence motor protein function during axonal transport. Other studies done in cultured cells found that GSK-3 β activity increased either in the presence of a FAD-linked PS mutation or with loss of PS function, leading to the proposal that de-regulation of GSK-3 β activity by loss of PS or familial AD-linked PS mutations can impair axonal transport (13,14). Further, increased GSK-3 β activity appeared to increase the levels of kinesin light chain (KLC) phosphorylation leading to a reduction in membrane bound kinesin-1, disrupting anterograde transport (13,14). Intriguingly, kinesin heavy chain (KHC), the motor domain that interacts with microtubules (MTs) for motility is also phosphorylated (15,16) and KHC phosphorylation also induces membrane association (15). However, whether GSK-3 β -mediated phosphorylation events on motor proteins control motor function during axonal transport *in vivo* and what role PS plays in this pathway remain allusive.

On the other hand, since GSK-3 β is a tau kinase (17), perhaps the observed GSK-3 β and PS-mediated effects on transport could arise due to abnormal tau function and associated MT defects. While excess of tau bound to MTs can physically impair axonal transport (18), destabilization of MTs by loss of tau function may also affect axonal transport. *In vitro* experiments found that the amount of tau associated with MTs can differentially modulate kinesin and dynein activities (19). Moreover, while tau phosphorylation can regulate its association with motor machinery (20), reductions in axonal transport mediated by kinesin can exacerbate tau hyperphosphorylation (21). However, whether PS also influences tau function and how MT abnormalities contribute to the observed transport defects remain unclear.

Here, we used genetics, *in vivo* and biochemical analysis in a simple model system to directly test the hypothesis that PS and GSK-3 β function together during axonal transport. Our observations show that PS influences GSK-3 β -activity during axonal transport via a pathway that affects both kinesin-1 and dynein function, but not tau. Our results propose a model in which PS may function to modulate GSK-3 β activity, which may influence kinesin-1 and dynein membrane binding, perhaps by controlling proper motor function during fast axonal transport.

RESULTS

PS genetically interacts with GSK-3 β during axonal transport

One simple prediction of the hypothesis that PS influences GSK-3 β -mediated roles during axonal transport is that PS and GSK-3 β should functionally interact with each other. To test this prediction, we analyzed *Drosophila* larvae carrying mutations of both the *Drosophila* homolog of GSK-3 β , Shaggy (sgg) and PS (psn). Previous work demonstrated that *Drosophila* larvae containing mutations in genes encoding motor proteins show dramatic neuromuscular pathology and flip their tails (22,23). The segmental nerves from these mutant larvae contained prominently stained accumulations of synaptic vesicle proteins such as synaptotagmin (SYT) and cysteine string protein (CSP) (22,23). These synaptic accumulations are referred to as the axonal blockage phenotype. This phenotype

which can be observed both in fixed (23–29) or live larval preparations (25,28,30) has successfully led to the identification of several novel genes involved in axonal transport (25,26,31). Under transmission EM, many types of identifiable axonal cargo (mitochondria, clear vesicles, dense core vesicles, large multi-vesicular bodies and large, dark prelysosomal vacuoles) are observed within these axonal swellings (22,23,28).

The *Drosophila* sgg gene shares >90% sequence similarity with human GSK-3 β with the greatest similarity seen within the kinase domain (17). Sgg is also regulated by phosphorylation similar to human GSK-3 β (4). Most loss-of-function mutations of sgg results in embryonic or larval lethality and do not eclose to adults. We used two loss-of-function sgg mutations; the amorphic loss-of-function mutant sgg^[M11], which is a well-characterized spontaneously occurring mutation that causes death during embryogenesis (32), and the X-ray-induced amorphic early larval lethal mutant sgg^[1] (17). Larvae heterozygous for sgg^[M11]–/+ or sgg^[1]–/+ do not show detectable levels of axonal blocks and are comparable with WT (Fig. 1A and B).

Unlike mammals, *Drosophila* has one PS gene, which produces two alternatively spliced forms. *Drosophila* PS is ~50% amino acid sequence identity to human PS (33–35) and loss-of-function PS mutations result in lethal notch-like phenotypes (36,37). Similar to mammalian PS, two intramembranous aspartate residues are conserved in *Drosophila* PS (33,35). We used two loss-of-function mutations in the *Drosophila* PS gene; the amorphic psn^[2] mutation is a point mutation that produces a truncated product ending at W278 (37,38) causing a null mutation that results in death at early larval stages, and the psn^[143], which is a deletion and/or splice site mutation resulting in the deletion of amino acids between the first transmembrane domain and the middle of the fourth transmembrane domain (Annette Parks communication to Flybase). This psn^[143] encodes a loss-of-function mutation and results in death at late larval stages. Quantitative PCR analysis confirmed that heterozygous combinations of psn^[2]–/+ or psn^[143]–/+ larvae express reduced amounts of PS mRNA compared with WT larvae (12). Homozygous psn^[143]–/– larvae or heterozygous psn^[143]–/+ or the psn^[2]–/+ larvae do not show detectable levels of axonal blocks and were comparable with WT, similar to our previous observations (Fig. 1A, C, E, (12)). These observations are similar to what was seen in larvae with reductions of kinesin-1 or dynein, and only larvae containing complete loss of function of motors showed axonal transport defects (22–24).

To test the prediction that PS and GSK-3 β functionally interact with each other, we generated larvae that contained 50% reduction of SGG and 50% reduction of PS. The amorphic sgg alleles sgg^[M11] or sgg^[1] were crossed to amorphic PS alleles, psn^[2] or psn^[143]. We observed large amounts of axonal accumulations that contained CSP in nerves from larvae containing 50% reduction of SGG and 50% reduction of PS (sgg^[M11]–/+; psn^[2]–/+, Fig. 1D or sgg^[M11]–/+; psn^[143]–/+, Fig. 1F). Quantification analysis indicated that the number of blockages in these larvae (sgg^[M11]–/+; psn^[2] or sgg^[M11]–/+; psn^[143]–/+) was significantly increased compared with WT, heterozygous sgg (sgg^[M11]–/+) or psn larvae (psn^[2] or psn^[143]–/+, Fig. 1G, $P < 0.001$). Larvae that were sgg^[1]–/+; psn^[2]–/+ or sgg^[1]–/+; psn^[143]–/+ also showed significant amounts of axonal blocks (Fig. 1G, $P < 0.001$). The extent of

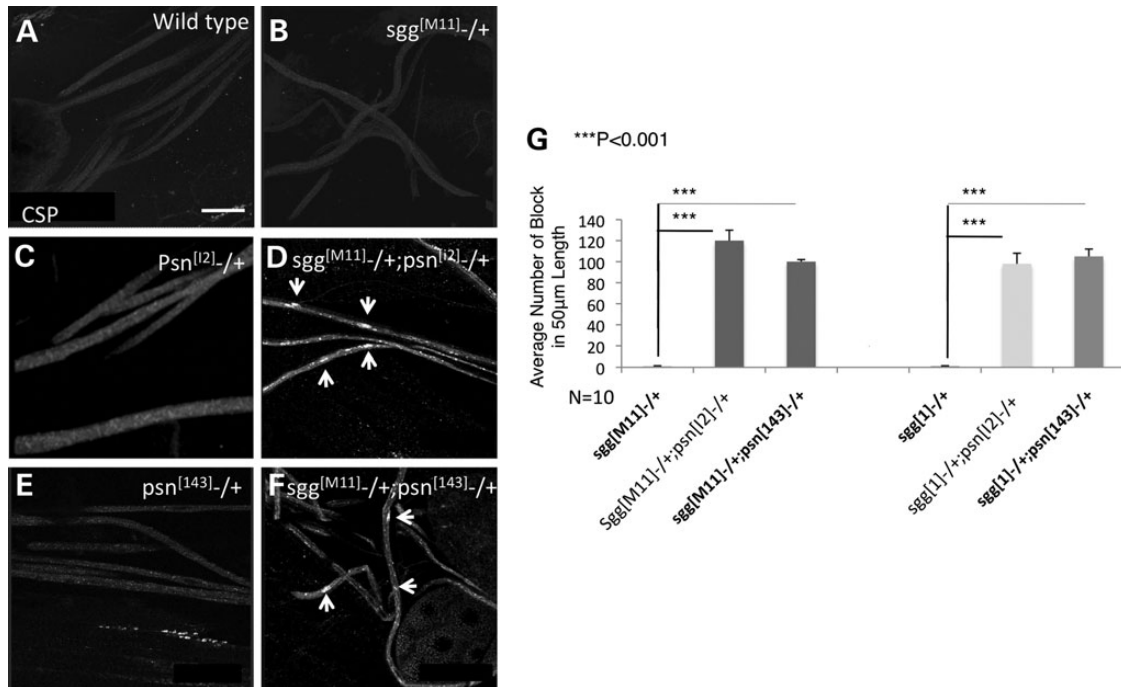


Figure 1. PS genetically interacts with GSK-3 β . Heterozygous *sgg*^{[M11]-/+} (B), *psn*^{[12]-/+} (C) or *psn*^{[143]-/+} (E) larvae do not show axonal blockages and were comparable with WT larvae (A). Fifty percentage reduction of SGG with 50% reduction of PS (*sgg*^{[M11]-/+;psn^{[12]-/+}, (D), or *sgg*^{[M11]-/+;psn^{[143]-/+}, (F) showed a significant amount of axonal blockages (arrows). (G) Quantification analysis indicated a statistically significant increase in the amount of axonal blockages with 50% reduction of PS (*sgg*^{[M11]-/+;psn^{[12]-/+} or *sgg*^{[M11]-/+;psn^{[143]-/+}, $P < 0.001$) compared with *sgg*^{[M11]-/+}, or *psn*^{[12]-/+} or *psn*^{[143]-/+} alone. Similar results were seen in *sgg*^{[11]-/+;psn^{[12]-/+} or *sgg*^{[11]-/+;psn^{[143]-/+} larvae ($P < 0.001$). $N = 10$ for each genotype. Bar = 10 μ m.}}}}}}

axonal blockages in these larvae was comparable with what was seen in larvae with complete loss of function of kinesin-1 or dynein (22–24). These observations suggest that GSK-3 β and PS have an important functional relationship during axonal transport.

Since GSK-3 β is a tau kinase, and tau is an MT-binding protein, it is possible that the axonal blockages we observed arose due to PS-dependent GSK-3 β -mediated effects on tau. In this context, at least two possibilities could exist to cause these axonal defects: (i) changes in tau–MT interactions affecting MT stability could lead to blockages (39–41), and/or (ii) changes in tau phosphorylation could affect motor protein motility (20,21,42–45) causing blockages. To test these, we examined the stability of axonal MTs *in vivo* in the context of reduction of GSK-3 β or reduction of PS using hTAU-GFP. Larvae expressing hTAU-GFP showed smooth GFP MT tracks (Supplementary Material, Fig. S1A), which also stained with Futsch, an MT-binding protein and acetylated tubulin (Supplementary Material, Fig. S1G and H). Motility of mRFP-tagged vesicles was observed moving along these GFP tracks (Supplementary Material, Fig. S1F). Although it was unclear as to how much of the expressed hTAU-GFP was bound to endogenous MTs, we were able to readily observe fragmented MTs under conditions of injury (Supplementary Material, Fig. S1B) similar to previous observations (46). However, reduction of PS or GSK-3 β did not cause fragmented MTs as assayed *in vivo* in hTAU-GFP; *psn*^{[12]-/+} (Supplementary Material, Fig. S1I) or hTAU-GFP;*sgg*^{[M11]-/+} (Supplementary Material, Fig. S1J) larval axons. Moreover, excess of GSK-3 β also did not cause fragmented MTs (hTAU-GFP;*sgg*^{WT}, Supplementary Material,

Fig. S1K). Further, our observations were consistent with a recent study that showed that only complete loss of GSK-3 β altered MT stability, while reduction or over expression of GSK-3 β had no effect on MTs (11). Therefore, while a complete loss of GSK-3 β led to increased MT stability (11) and reduction of GSK-3 β or PS did not have an observable effect on MTs (Supplementary Material, Fig. S1) despite impairing transport, the PS-dependent GSK-3 β -mediated transport defects we observed may not be primarily caused by MT abnormalities. However, whether the observed transport defects were due to PS-dependent changes on GSK-3 β -mediated tau phosphorylation remains unclear and needs further investigation.

PS influences active GSK-3 β during axonal transport

Several signaling pathways have been found to regulate GSK3 β activity by upstream regulators in response to stimuli (3). Similarly, PS may function as an upstream regulator that modulates GSK-3 β activity during axonal transport. Indeed, previous work in cultured cells found that loss of function of PS or a mutation in PS increased phosphorylation of KLC by influencing GSK-3 β activity, leading to a reduction of membrane bound kinesin-1 (13,14), postulating that PS may function to modulate GSK-3 β activity during axonal transport. One prediction of this proposal is that loss of PS should stimulate GSK-3 β activity. To test this, we used biochemical analysis to evaluate GSK-3 β activity in heterozygous PS larvae (*psn*^{[12]-/+}), since null mutants of PS die at early larval stages. In contrast to previous observations in cells, we found that the level of active GSK-3 β was significantly decreased in the postnuclear supernatant

(PNS) of $psn^{[12]-/+}$ larvae compared with WT larvae (Fig. 2A and B, $P < 0.005$). Reduction of PS also decreased the amount of membrane bound active GSK-3 β (Fig. 2A and B, $P < 0.05$). Strikingly, the amount of kinesin-1 and dynein bound to membranes was also decreased in $psn^{[12]-/+}$ membranes compared with WT membranes (Fig. 2A and B, ($P < 0.05$), suggesting that the binding of motors to membranes may be dependent on PS and active GSK-3 β . Consistent with this, the amount of kinesin-1 and dynein in the soluble fraction was increased with reduction of PS (Supplementary Material, Fig. S2). Collectively, our results suggest that under physiological conditions PS can function to modulate GSK-3 β activity to influence both kinesin-1 and dynein motor binding to membranes. Therefore, decreases in membrane bound motors mediated by reduction of GSK-3 β activity could cause the axonal transport defects observed in $sgg^{-/+}$; $psn^{-/+}$ larvae (Fig. 1D and F).

The proposal that GSK-3 β activity is necessary for axonal transport leads to the prediction that excess of active GSK-3 β should perturb axonal transport by increasing motor binding to membranes. Indeed, excess of SGG^{ACTIVE} but not excess of a kinase-dead or non-functional form of SGG (SGG^N) caused axonal transport defects (Fig. 3A–D). Similarly, excess of SGG^{WT}, which had increased levels of active GSK-3 β , also caused axonal transport defects (Fig. 3A and D). Excess of active GSK-3 β was observed in both the PNS and the membrane fraction of larval brains expressing SGG^{ACTIVE} or SGG^{WT} compared with WT larval brains (Fig. 4A and data not shown).

To biochemically confirm that increased GSK-3 β activity increases motor binding to membranes, we evaluated the amount of motor proteins bound to membranes in brains expressing SGG^{ACTIVE} and compared these levels with the levels observed in WT (Fig. 4A). Quantification of three independent experiments revealed a two- to three-fold increase of kinesin-1 in membranes from SGG^{ACTIVE} brains compared with WT brains ($P < 0.05$), while no significant change was seen in the level of kinesin-1 in the PNS (Fig. 4A). Intriguingly, we also observed a significant increase in the level of dynein bound to membranes from SGG^{ACTIVE} brains compared with WT brains ($P < 0.05$, Fig. 4A). Similar observations were also seen in brains expressing SGG^{WT} (data not shown). In contrast, significant decreases were observed in the level of kinesin-1 and dynein in membranes from mutant $sgg^{[M11]-/+}$ compared with WT brains ($P < 0.05$, Fig. 4B). Taken together, our results indicate that the activity of GSK-3 β is required for motor protein binding to membranes. Therefore, excess GSK-3 β activity can perturb axonal transport by increasing the amount of motors on moving vesicles.

PS-dependent GSK-3 β activity negatively controls motor function during axonal transport

The proposal that PS influences GSK-3 β activity leads to the prediction that reduction of PS in the context of excess GSK-3 β should suppress GSK-3 β activity-dependent transport

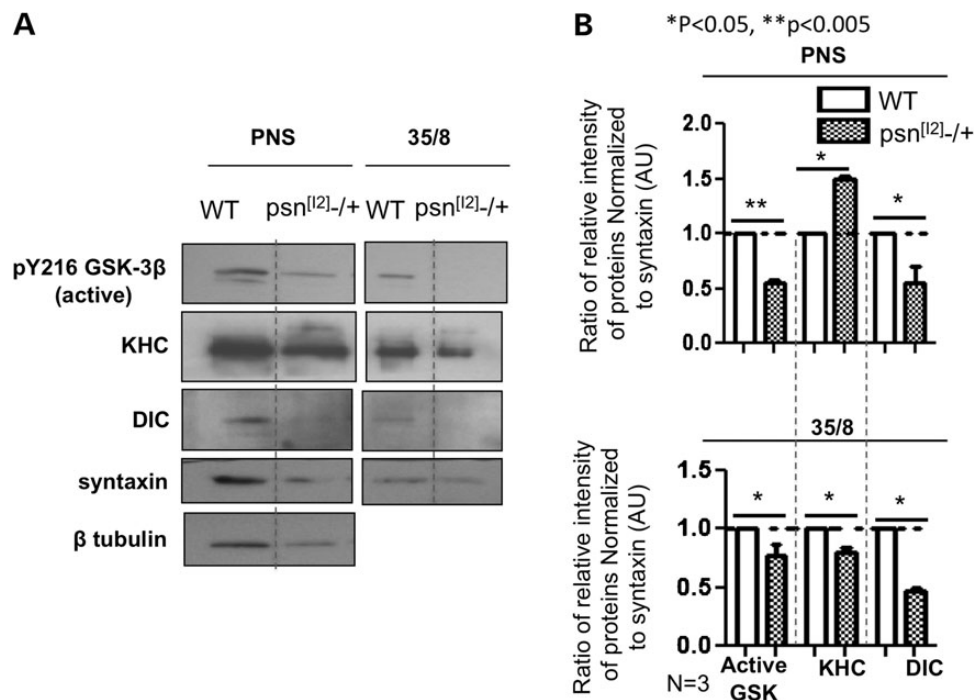


Figure 2. Reduction of PS decreases membrane binding of active GSK-3 β . (A) Subcellular fractionation of third instar larval brain membranes on sucrose step gradients indicated that reduction of PS ($psn^{[12]-/+}$) decreased the level of active GSK-3 β that was associated with light membranes (membrane fraction, 35/8) compared with WT brains. The antibody against active GSK-3 β (pY216 GSK-3 β) was used. Note that this observation was similar to what was seen with reduction of sgg ($sgg^{[M11]-/+}$, Fig. 4F). The levels of KHC and DIC were also decreased in the membrane fraction from $psn^{[12]-/+}$ brains compared with WT brains. (B) Quantification analysis indicated that the extent of the decrease seen in active GSK-3 β , KHC or DIC in the 35/8 fraction was statistically significant ($*P < 0.05$, $**P < 0.005$). The ratio of relative intensity of proteins normalized to syntaxin is shown from three independent experiments. For quantification analysis of the PNS fraction, the ratio between the intensity of active GSK-3 β and the intensity of syntaxin was determined and normalized to WT, and the level of intensity in WT was set at 1. For quantification analysis of the 35/8 membrane fraction, the ratio between the intensity of KHC/DIC/active GSK-3 β and the intensity of syntaxin was determined and normalized to WT. Y-axis depicts the intensity in arbitrary units (AUs). $N = 3$.

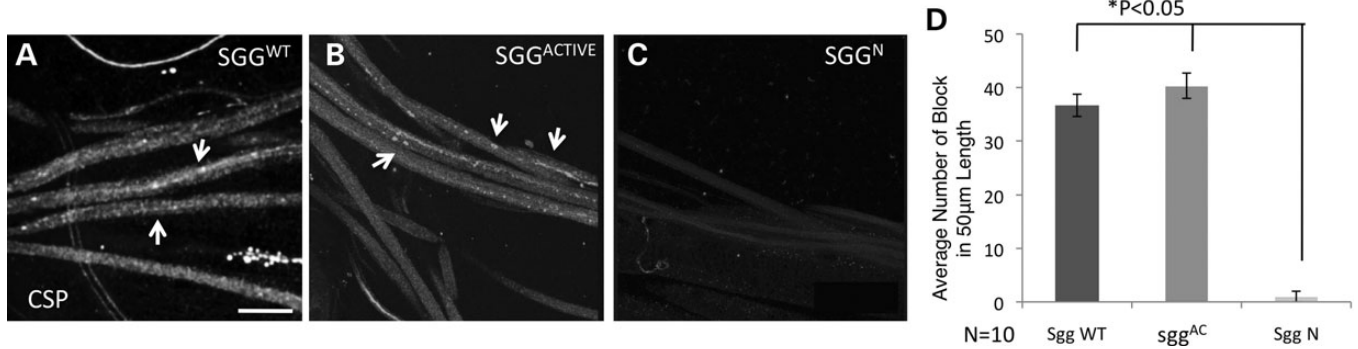


Figure 3. Active GSK-3 β is necessary for axonal transport. Larval segmental nerves from larvae expressing WT SGG (SGG^{WT}, (A) or active SGG (SGG^{ACTIVE}, (B) showed many axonal blockages (arrows) in contrast to larvae expressing a non-functional form of SGG (SGG^N, C). (D) Quantification analysis indicated that the extent of axonal blockages in larvae expressing SGG^{WT} and SGG^{ACTIVE} was statistically significant compared with larvae expressing a non-functional form of SGG ($P < 0.05$, $N = 10$ larvae for each genotype). Bar = 10 μ m.

defects by decreasing motor binding to membranes. In contrast to this prediction, we found that 50% reduction of PS with excess of SGG^{ACTIVE} failed to suppress axonal blocks (Fig. 5A–C), but instead caused an enhancement of axonal blockages compared with larvae expressing SGG^{ACTIVE} alone. Enhanced axonal blockages were observed in both SGG^{ACTIVE}; *psn*^[12]–/+ or SGG^{ACTIVE}; *psn*^[143]–/+ larvae (Fig. 5B and C). These larvae also showed the characteristic tail flip phenotype and did not eclose to adults (data not shown). Reduction of PS had no effect on the kinase-dead or non-functional form of GSK-3 β (SGG^N, Fig. 5D and E). Quantitative analysis revealed that the number of blockages in SGG^{ACTIVE}; *psn*^[12]–/+ and SGG^{ACTIVE}; *psn*^[143]–/+ larvae was significantly increased compared with SGG^{ACTIVE} alone ($P < 0.001$, Fig. 5F). Similar observations were also seen in SGG^{WT}; *psn*^[12]–/+ and SGG^{WT}; *psn*^[143]–/+ larvae (Fig. 5F). The extent of blockages in these larvae was comparable with the extent of axonal defects seen with complete loss of function of motor proteins (27). Collectively, these observations suggest that while GSK-3 β activity is important for motor binding to membranes, active GSK-3 β may also influence the proper control of motor protein function during vesicle motility *in vivo*. Indeed, recent work has suggested that GSK-3 β and PS may act as negative regulators to control the number of active motors that are moving cargoes *in vivo* (11,12). Therefore, reduction of PS in the context of excess active GSK-3 β may enhance axonal transport defects by improperly regulating motor protein function during cargo motility.

Although *in vitro* studies suggest that the binding of motors to membranes activates motor function (13), it is unclear how motor activity is initiated or controlled *in vivo*. The proposal that PS may influence GSK-3 β -activity-dependent control of motor proteins leads to the prediction that activity changes in GSK-3 β should significantly affect vesicle motility during transport. Therefore, both decreases and increases in GSK-3 β activity should significantly influence vesicle velocities *in vivo*. Indeed, consistent with this proposal, reduction of PS decreased GSK-3 β activity (Fig. 2), but increased both the anterograde and retrograde vesicle velocities (12) likely by improperly regulating motors. Similarly, reduction of GSK-3 β also increased both the anterograde and retrograde vesicle velocities (11). Furthermore, excess of GSK-3 β significantly decreased the average anterograde and retrograde duration-weighted

segmental velocities of synaptobrevin vesicles (synb-GFP) or mitochondria (mito-GFP), two vesicles/organelles transport by kinesin-1 in the context of excess GSK-3 β (Fig. 6A and B, Supplementary Material, Fig. S3A–D and Table S1, $P < 0.001$ (47,48). In larvae expressing excess SGG^{WT}, the average velocities of synaptobrevin vesicles significantly decreased to 0.118 and 0.099 μ m/s from 0.283 and 0.294 μ m/s in the anterograde and retrograde directions, respectively (Fig. 6C and D, Supplementary Material, Fig. S3A and B, $P < 0.001$; Supplementary Material, Table S1 and Movies S1 and S2). In larvae expressing excess SGG^{WT}, the average velocities of mitochondria significantly decreased to 0.364 and 0.233 μ m/s from 0.511 and 0.457 μ m/s in the anterograde and retrograde directions, respectively (Fig. 6E and F, Supplementary Material, Fig. S3C and D, $P < 0.001$, Supplementary Material, Table S1 and Movies S3 and S4). Similar to our observations, Weaver *et al.* (11) also reported that excess GSK-3 β decreased both the anterograde and retrograde velocities of APP vesicles, another vesicle transported by kinesin-1.

Substantial changes in pause durations, pause frequency and run lengths were also observed, indicating that vesicle velocity changes can occur due to changes in the frequency and duration of vesicle pauses causing changes in vesicle runs. Significant increases were seen in retrograde pause duration and pause frequency ($P < 0.05$), and in the anterograde pause frequency ($P < 0.005$) in synb-GFP, while only a mild change was detected in the anterograde pause duration in synb-GFP in larvae expressing SGG^{WT} compared with larvae containing normal levels of SGG ($P = 0.0647$, Fig. 6G–J). Significant increases in retrograde pause duration and pause frequency were observed in mito-GFP, while no significant changes were detected in anterograde pause duration or pause frequency in mito-GFP in larvae expressing SGG^{WT} compared with larvae containing normal levels of SGG (Fig. 6G–J). Consistent with the prediction that increased vesicle pausing should decrease vesicle run lengths, significant decreases in the anterograde synb-GFP ($P < 0.05$) and retrograde mito-GFP ($P < 0.05$) run lengths were seen in larvae expressing SGG^{WT} compared with larvae containing normal levels of SGG (Fig. 6K and L), while a trend toward decreased run lengths were seen in retrograde synb-GFP ($P = 0.158$) and anterograde mito-GFP ($P = 0.063$). Such changes in the motility of synaptobrevin vesicles or

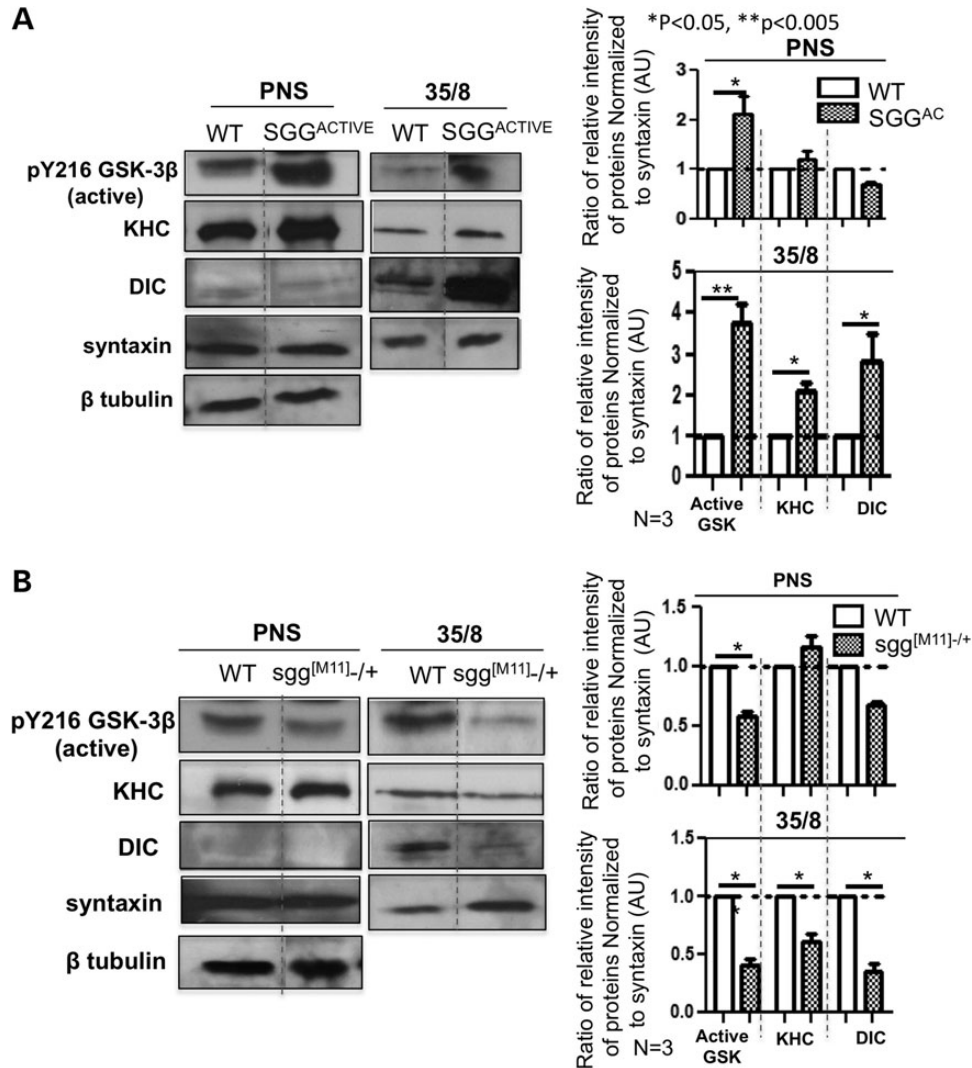


Figure 4. Active GSK-3 β influences kinesin-1 and dynein binding to membranes. (A) Subcellular fractionation of third instar larval brain membranes on sucrose step gradients indicated that expression of SGG^{ACTIVE} increased the level of active GSK-3 β that is associated with light membranes (membrane fraction, 35/8) compared with WT brains. Note that the levels of KHC and DIC were also increased in the membrane fraction from brains expressing SGG^{ACTIVE} compared with WT brains. Quantification analysis indicated that the extent of the increase seen in active GSK-3 β , KHC or DIC in the 35/8 fraction was statistically significant (* $P < 0.05$, ** $P < 0.005$, $N = 2-3$). Y-axis depicts the intensity in AUs. (B) In contrast, reduction of SGG (sgg^{[M11]-/+}) decreased the level of active GSK-3 β that is associated with light membranes compared with WT. The levels of KHC and DIC were also decreased in sgg^{[M11]-/+} membranes. Quantification analysis indicated the decrease seen in active GSK-3 β , KHC or DIC in the 35/8 fraction was statistically significant (* $P < 0.05$, ** $P < 0.005$, $N = 3$).

mitochondria could be due to changes in motor protein function. Indeed, cargo population analysis showed increased stalled or static vesicles/organelles with excess SGG compared with normal SGG, consistent with decreased populations of anterograde, retrograde or reversing vesicles/organelles (Supplementary Material, Fig. S2E and F). The significant increases in both synb-GFP and mito-GFP ($P < 0.05$) switch frequencies observed in larvae expressing SGG^{WT} compared with larvae containing normal levels of SGG (Fig. 6M) suggest that the correlative coordination of kinesin-1 and dynein motor function on synaptobrevin vesicles and mitochondria could be disrupted. Therefore, taken together these observations suggest that GSK-3 β activity can negatively influence the coordinated function of both kinesin-1 and dynein motor function on vesicles during motility on MTs, and that this role may also be dependent on PS. Consistent with this, we found that reduction of motors

with excess active GSK-3 β enhanced axonal transport defects (Supplementary Material, Fig. S3). Therefore, while excess GSK-3 β increases motor binding to membranes, motor function activities on vesicles are negatively regulated causing improper motor function and motility defects (Supplementary Material, Fig. S6).

DISCUSSION

We have identified a novel physiological role for PS and GSK-3 β during axonal transport using genetics, *in vivo* imaging and biochemical analysis in *Drosophila*. Specifically, our observations lead us to two major conclusions: (i) PS and GSK-3 β functionally interact with each other during axonal transport, and (ii) PS influences GSK-3 β -activity for proper

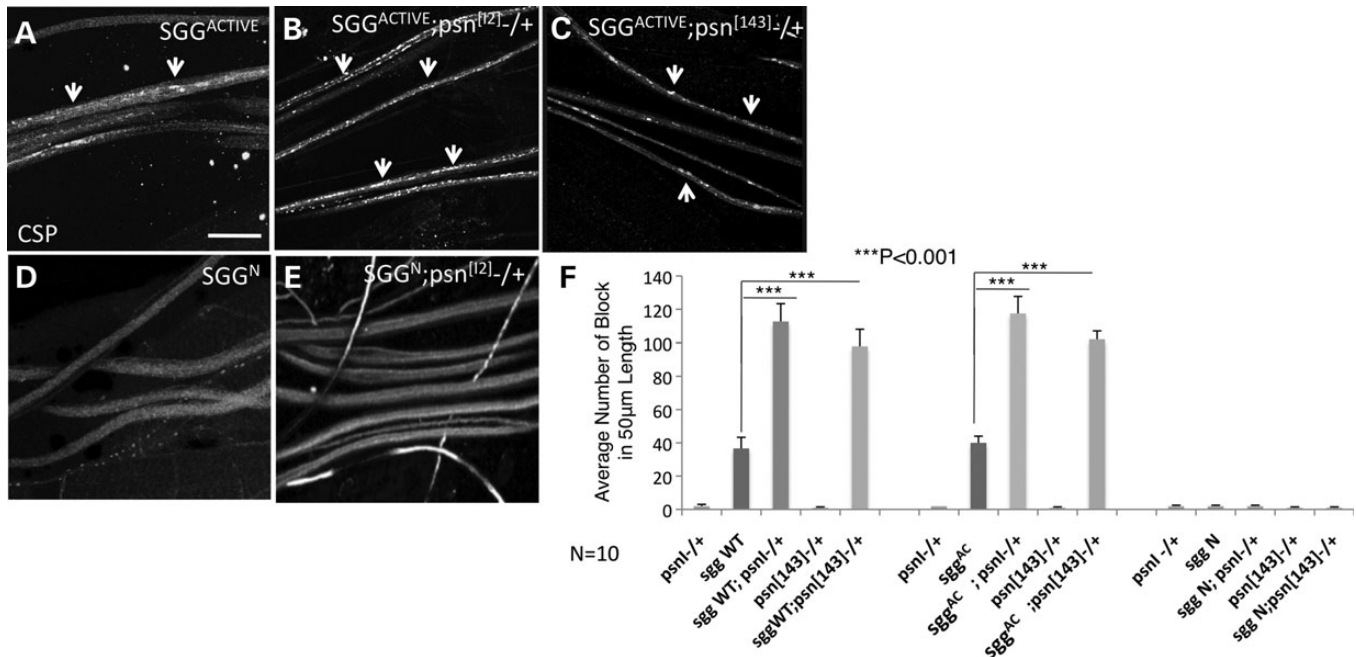


Figure 5. PS influences GSK-3 β activity-dependent motor protein function during axonal transport. (A) Excess of SGG^{ACTIVE} alone caused axonal defects, but excess of a non-functional SGG^N (D) does not. Fifty percent reduction of PS increased axonal blockages mediated by excess of SGG^{ACTIVE} (B, SGG^{ACTIVE}; psn^[12]-/+; arrows), while expression of the non-functional SGG with 50% reduction of PS had no effect (E, SGG^N; psn^[12]-/+). Increased axonal blockages were also seen in SGG^{ACTIVE}; psn^[143]-/+ (C). (F) Quantification analysis indicated that 50% reduction of PS significantly increased the number of GSK-3 β -mediated blockages in SGG^{ACTIVE}; psn^[12]-/+, SGG^{ACTIVE}; psn^[143]-/+, SGG^{WT}; psn^[12]-/+ or SGG^{WT}; psn^[143]-/+ larvae compared with SGG^{ACTIVE} or SGG^{WT} larvae ($P < 0.001$). No effect was seen in SGG^N; psn^[12]-/+ or SGG^N; psn^[143]-/+ larvae. $N = 10$ for each genotype. Bar = 10 μ m.

axonal transport via a pathway that affects both kinesin-1 and dynein function. These findings have important implications for our understanding of the complex regulatory machinery that is involved in the movement of vesicles by both kinesin-1 and dynein motors *in vivo*.

PS modulates GSK-3 β activity during axonal transport

In vitro studies previously suggested that PS may influence GSK3 β activity to affect kinesin-1-mediated axonal transport (13,14). Consistent with this proposal, we found that GSK-3 β and PS functionally interacts with each other in the context of axonal transport *in vivo*. Our genetic analysis showed that while reduction of GSK-3 β or PS alone did not cause axonal transport defects, reduction of both GSK-3 β and PS caused axonal blockages (Fig. 1). There are at least three possibilities to explain the cause of these axonal transport defects. One possibility is that both PS and GSK-3 β function together during axonal transport via an action on motors. PS is transported bi-directionally within PNS and CNS axons (49–51), and is contained within APP vesicles (52). *In vivo*, reduction of PS altered both the anterograde and retrograde velocities of vesicles by influencing both kinesin-1 and dynein motors (12). While the transport of GSK-3 β has not been directly observed, GSK-3 β is present in neurons and neuronal membranes that contain kinesin-1 (13,14) (Fig. 4) and dynein (Fig. 4). Similar to PS, GSK-3 β also influences both anterograde and retrograde vesicle velocities *in vivo* (11). Since reduction of PS decreased GSK-3 β activity and kinesin-1 and dynein binding to membranes (Fig. 2), and excess active GSK-3 β decreased vesicle

velocities by increasing pause frequencies/durations and switch frequencies, and decreasing run lengths (Fig. 6), perhaps PS functions to modulate GSK-3 β activity for cooperative and coordinated kinesin-1 and dynein motor function during transport (Supplementary Material, Fig. S6).

The second possibility is that the PS and GSK-3 β -mediated axonal blockages we observed could result due to defects in MT stability. However, reduction of GSK-3 β or PS, or excess of GSK-3 β did not cause any observable change in MT stability as assayed using Tau-GFP despite impairing transport (Supplementary Material, Fig. S1; Figs 1 and 3). Similarly, recent observations using EB1-GFP also failed to detect MT defects with reduction or excess of GSK-3 β (11). Perhaps, subtle changes in MTs could exist that escaped our analysis, which could impact vesicle motility leading to transport defects.

A third possibility is that PS may influence GSK-3 β -mediated tau-dependent axonal transport defects in a phosphorylation-dependent manner. Mechanistically, GSK-3 β -mediated tau-dependent transport defects could arise due to changes in the phosphorylation state of tau and the amount of tau associated with MTs, which could interfere with the binding of kinesin-1 and dynein motors to MTs (19,20,44). Indeed, Mudher *et al.* (18) found that excess active GSK-3 β can enhance tau-dependent axonal defects, but this study did not assess the biochemical activity of GSK-3 β or the binding of motors to MTs. Although currently little is known about a role for PS in GSK-3 β -mediated tau phosphorylation, perhaps most likely some combination of these events led to the axonal transport defects we observed. While further studies would be needed to evaluate the contribution of each of these factors, our work raises the possibility that

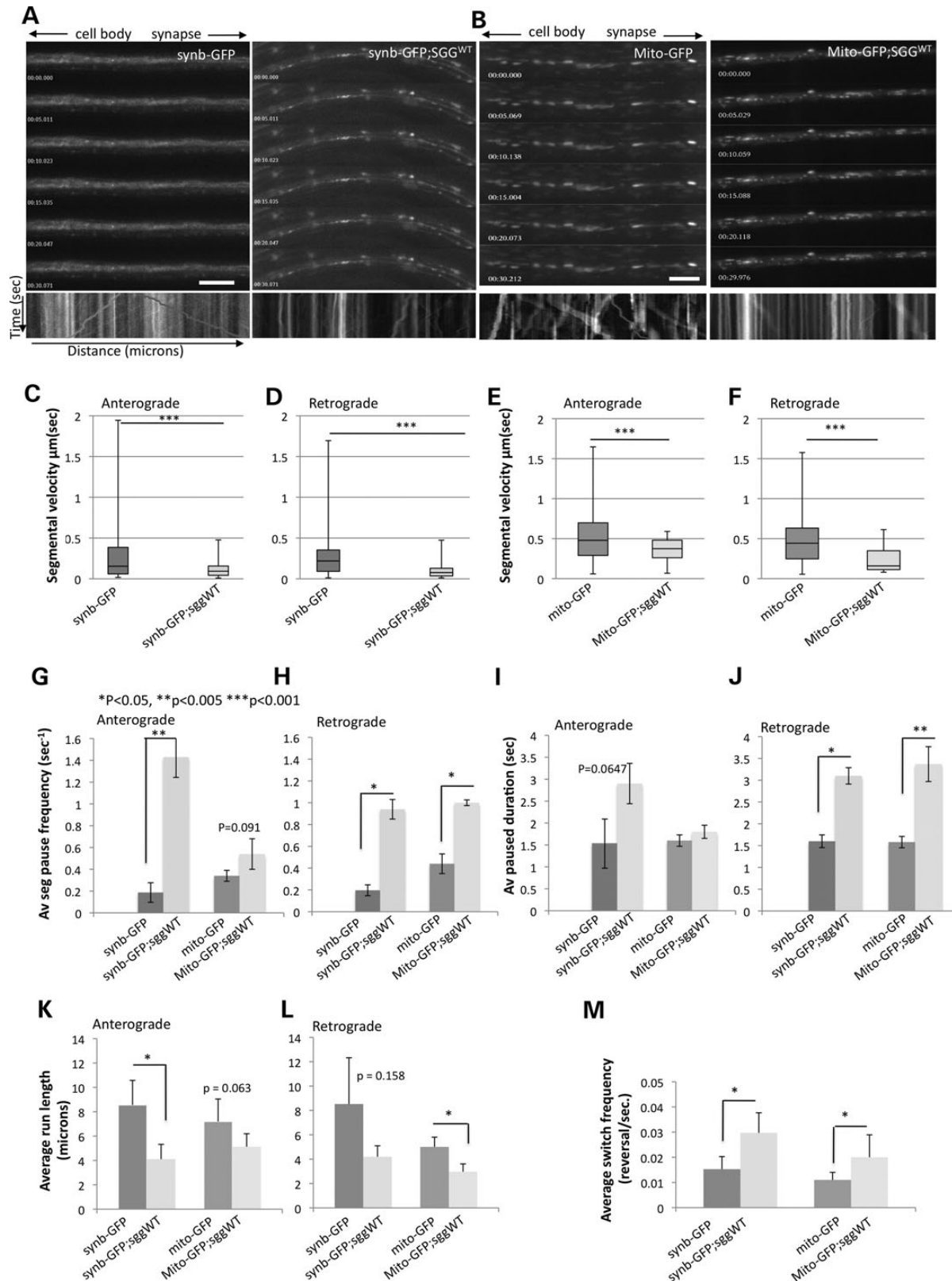


Figure 6. Excess of GSK-3 β activity perturbs the movement of synaptobrevin vesicles and mitochondria *in vivo*. (A) A montage from a representative movie (Supplementary Material, movie S1) shows diffused synb-GFP with faint bidirectionally moving vesicles from a larvae expressing synb-GFP. The representative kymograph shows robust bidirectional movement with synb-GFP vesicles (red line = anterograde, green line = retrograde). Cell bodies are toward the left and the synapse is toward the right as depicted by the arrows at the top. In contrast, expression of SGG^{WT} perturbed the movement of synb-GFP causing synb-GFP blocks (Supplementary Material, Movie S2). The kymograph shows stalled blockages. On the kymograph, the Y-axis depicts the time and the X-axis depicts the distance.

defects in regulatory pathways mediated by PS and GSK-3 β directly impairs vesicle transport *in vivo*.

Is motor protein function influenced by GSK-3 β phosphorylation?

It is possible that phosphorylation plays a key role in the regulation of motor protein activity and function. Previous work in cells suggested that the binding of kinesin-1 to membranes was dependent on the phosphorylation state of KLC, which is thought to be controlled by GSK-3 β (14,16). While our *in vivo* findings also suggest that GSK-3 β activity influenced membrane binding of motor proteins (Fig. 4), GSK-3 β activity appears to also influence motor protein function (Fig. 6), perhaps via phosphorylation events. Although both KHC and KLC are phosphorylated under physiological conditions (15,53), the exact identity of the kinase(s) responsible for this action and the role differential phosphorylation of kinesin-1 subunits play in motor function are unclear. Furthermore, both KLC and KHC contain AMPK phosphorylation sites, in addition to GSK-3 β phosphorylation sites (54). Sites for other kinases are also present on both KLC and KHC (53,55), indicating that phosphorylation of kinesin-1 and its subunits can play an important role in regulating its motor function *in vivo* (56). Unlike mammalian KLC, the protein sequence of *Drosophila* KLC lacks the XSXXSX GSK-3 β phosphorylation consensus sequence (57), while *Drosophila* KHC has two putative GSK-3 β phosphorylation sequences. One of these putative sequences is within the kinesin motor domain and the other is within the stalk. Intriguingly, Lee *et al.* (15) previously proposed that phosphorylation of KHC, not KLC was required to induce membrane association, indicating that phosphorylation of KHC could influence membrane binding or motor function or both. Since we found that active GSK-3 β influenced both motor binding to membranes (Fig. 4) and motor function (Fig. 6), perhaps GSK-3 β -dependent phosphorylation of KHC could dictate the balance between these roles. It is conceivable that differential phosphorylation of the sites in the motor or stalk domains may coordinate the regulation of these functions. Although further study is needed to test these predictions, it is clear that under physiological conditions, GSK-3 β plays an important role in controlling kinesin-1 function *in vivo*.

Our results also provide the first direct evidence for GSK-3 β in regulating dynein-mediated transport. We found that GSK-3 β activity influenced dynein binding to membranes and dynein-mediated retrograde vesicle velocities (Figs 4 and 6), indicating that these actions could also be controlled by GSK-3 β -dependent phosphorylation of dynein. Indeed, phosphorylation has recently been shown to regulate targeting of cytoplasmic dynein to kinetochores during mitosis (58). A role for phosphorylation in the regulation of dynein light chain assembly has also been demonstrated (59). An early study reported that dynein associated with anterogradely moving organelles was phosphorylated, suggesting that differential phosphorylation could regulate dynein function (60). Intriguingly, *Drosophila* dynein heavy chain (DHC) has several putative GSK-3 β phosphorylation consensus sequences, including one in DHC's motor domain. Although further study is needed, perhaps GSK-3 β -dependent phosphorylation of dynein could dictate proper dynein motor function *in vivo*.

Does GSK-3 β control PS function during axonal transport?

Although we found that the GSK-3 β activity-mediated effects on transport were dependent on PS (Figs 1 and 5), it is possible that GSK-3 β may also control PS function during axonal transport and a feedback regulatory mechanism could exist under physiological conditions. Early work identified conserved GSK-3 β consensus phosphorylation sites on PS (61,62). Phosphorylation of PS at one of these GSK-3 β motifs mediated the interaction between PS and β -catenin (61), while phosphorylation at the second site altered the turnover of PS C-terminal fragment (CTF) (62). Moreover, endogenous GSK-3 β was found to be part of a tetrameric complex with PS-CTF/NTF and β -catenin, indicating that a GSK-3 β /PS complex plays an important role in the β -catenin pathway (63). Whether the PS-dependent GSK-3 β activity changes we observed during axonal transport were also mediated through complex formation between PS, GSK-3 β and motor proteins (64) remain to be examined.

In summary, our findings suggest that a complex regulatory mechanism exists *in vivo* and sheds new light on how this system is coordinated during the movement of vesicles within a living organism. Further, our work proposes that axonal transport defects induced by regulatory problems could contribute to

(B) A montage from a representative movie shows bidirectional movement of mitochondria in a larvae expressing Mito-GFP (Supplementary Material, Movie S3). In contrast, expression of SGG^{WT} caused decreased movement of mitochondria, which are stalled in the representative kymograph (Supplementary Material, Movie S4). For each genotype, a total of five animals were imaged for data analysis; four time-lapsed movies were collected for each animal; a total of 20 movies were analyzed. Bar = 20 μ m. (C and D) Box plots of duration-weighted segmental velocities of synaptobrevin-GFP (synb-GFP) in larvae with normal SGG compared with larvae with excess SGG^{WT} showed that excess SGG significantly perturbed both anterograde ($P < 0.001$) and retrograde ($P < 0.001$) velocities of synb-GFP vesicle movement. Box plots outline the distribution of duration-weighted segmental velocities for each genotype. The horizontal bar represents the median. The upper and lower box edges represent 75% percentile (i.e. upper quartile) and 25% percentile (i.e. lower quartile), respectively. (E and F) Box plots of duration-weighted segmental velocities of mitochondria-GFP (Mito-GFP) in larvae with normal SGG compared with larvae with excess SGG^{WT} also showed that excess SGG significantly perturbed both anterograde ($P < 0.001$) and retrograde ($P < 0.001$) velocities of Mito-GFP. Data were analyzed from five larvae and a total of 20 movies, 4 movies from each larvae were used (Anterograde synb-GFP tracks/vesicles $n = 149$; synb-GFP;SGG^{WT} $n = 90$; retrograde synb-GFP tracks/vesicles $n = 114$; synb-GFP;SGG^{WT} $n = 53$. Anterograde Mito-GFP tracks/vesicles $n = 120$; Mito-GFP;SGG^{WT} $n = 30$; retrograde Mito-GFP tracks/vesicles $n = 123$; Mito-GFP;SGG^{WT} $n = 30$). (G, H) Significant increases were observed in the average segmental pause frequencies for both anterograde and retrograde vesicles from synb-GFP;SGG^{WT} larvae compared with synb-GFP larvae ($P < 0.05$ – $P < 0.005$), while significant increases were seen in retrograde vesicles from Mito-GFP;SGG^{WT} compared with Mito-GFP larvae ($P < 0.05$). (I and J) Significant increases in pause durations were seen in retrograde vesicles from synb-GFP;SGG^{WT} or Mito-GFP;SGG^{WT} larvae compared with synb-GFP or Mito-GFP larvae ($P < 0.05$ – $P < 0.005$). (K and L) Significant decreases in the average run lengths were seen for anterograde vesicles from synb-GFP;SGG^{WT} larvae compared with synb-GFP larvae ($P < 0.05$), while significant decreases were seen for retrograde vesicles from Mito-GFP;SGG^{WT} compared with Mito-GFP larvae ($P < 0.05$). The run length reports the distance a vesicle travels without pausing in microns (Y -axis). (M) Significant decreases in the average switch frequencies were seen for both synaptobrevin vesicles and mitochondria under excess SGG ($P < 0.05$). Switch frequency is defined as the number of reversals per second (times/s, Y -axis). Supplementary Material, Table S1 contains the summary of all *in vivo* measurements.

tau abnormalities, and neuronal and synaptic defects observed in Alzheimer's and tau disease pathology (28,65,66). Thus, our work could highlight a potential novel therapeutic pathway for early treatment, prior to neuronal loss and the occurrence of clinical symptoms of disease.

MATERIALS AND METHODS

Drosophila genetics

Two loss-of-function *Drosophila* Shaggy, *sgg*^[M-11] and *sgg*^[1], and two *Drosophila* PS, *psn*^[12] and *psn*^[143] mutants and three transgenic *Drosophila* GSK-3 β lines, UAS-SGGB (SGG^{WT}), UAS-SGGS9A (SGG^{ACTIVE}) and UAS-SGGKK83-84MI (SGG^N), were used (Bloomington Stock Center, (67)). For loss-of-function experiments, the KHC mutant, *khc*²⁰ and the dynein light chain mutant, *robl*^k, were used ((22–24). Expression of SGG^{WT}, SGG^{ACTIVE} or SGG^N was done by crossing these UAS lines to the pan neuronal GAL4 driver APPL-GAL4 (27) at 29°C. For genetic interaction experiments, APPL-GAL4;T(2:3) CyO TM6B, Tb/Pin^{88K} was used. The chromosome carrying T(2:3) CyO TM6B, Tb is referred to as B3 and carries the dominant markers, Hu, Tb and CyO. For genetic interaction tests with kinesin and dynein motors, APPL-GAL4/APPL-GAL4;B3/Pin^{88K} females were crossed to *khc*²⁰/T(2:3) CyO TM6B or *robl*^k/T(2:3) CyO TM6B, Tb males. Males that were APPL-GAL4/Y;*khc*²⁰/B3 or APPL-GAL4/Y;*robl*^k/B3 were crossed to females from the *sgg* transgenic lines and only females that were non-tubby were used for analysis. For genetic interaction tests with loss of function of *sgg*, *sgg*^[M-11] or *sgg*^[1] females were crossed to *khc*²⁰/T(2:3) CyO TM6B or *robl*^k/T(2:3) CyO TM6B, Tb males and females from this cross were used for analysis. For genetic interaction tests with PS, APPL-GAL4/APPL-GAL4;B3/Pin^{88K} females were crossed to *psn*^[12] or *psn*^[143]/TM6C, Tb males. Males that were APPL-GAL4/Y; *psn*^[12] or *psn*^[143]/B3 were crossed to females from the *sgg* transgenic lines (SGG^{WT}) or *sgg*^[1] or *sgg*^[M-11] and only females that were non-tubby were used for analysis. The transgenic human Tau line UAS-hTAU-GFP (Bloomington) was used. To evaluate MT stability males that were APPL-GAL4/Y; UAS-SGG^{WT} or APPL-GAL4/Y; *sgg*^[M-11]/B3 were crossed to virgin UAS-hTAU-GFP females and only females that were non-tubby was used for analysis.

Larval preparations, immunohistochemistry and quantification

Third instar larvae were dissected, fixed and segmental nerve immunostainings were done as described (68). Briefly, larvae were dissected in dissection buffer (2 × stock contains 128 mM NaCl, 4 mM MgCl₂, 2 mM KCl, 5 mM HEPES and 36 mM sucrose, pH 7.2). Dissected larvae were fixed in 4% formaldehyde and incubated overnight with antibodies against CSP (1:10, Developmental Studies Hybridoma Bank), GSK-3 β (1:100, Cell Signaling) and/or HRP-TR (1:100 Invitrogen). Larvae were incubated in secondary antibodies (Alexa anti-mouse 568 or Alexa anti-rabbit 488, 1:100, Invitrogen) and mounted using Vectashield mounting medium (Vector Labs). Images were collected using an Leica TCS SP2 AOBs Spectral

confocal microscope as described (27,68). Quantitative analysis on the extent of blockages was carried out by collecting six confocal optical images from larval neurons from the region directly below or posterior to the larval brain, where several segmental nerves are visible or come into focus through the optical series. For each genotype, four to six animals were imaged, and four nerves were analyzed over a length of 50 μ m, using the threshold, density slice and particle analysis functions in NIH image software as previously described (27).

In vivo microscopy of vesicle movement and MT integrity

Drosophila transgenic lines expressing synb-GFP, Mito-GFP or hTAU-GFP were generated as previously described (26,27). Females from this line were crossed to males from APPL-GAL4 or D42GAL4, which express in all neurons. Female larvae were used for all *in vivo* imaging. To generate D42GAL4;synb-GFP/SGG^{WT} larvae, females that were D42;synb-GFP were crossed to males that were SGG^{WT}/B3 and non-tubby female larvae that were D42GAL4;synb-GFP/SGG^{WT} were used. To generate APPL-GAL4;Mito-GFP/SGG^{WT} larvae, females that were APPL-GAL4;SGG^{WT}/B3 were generated and crossed to Mito-GFP males and non-tubby female larvae from this cross was used for *in vivo* analysis. To express APPL-GAL4;hTAU-GFP/SGG^{WT}, APPL-GAL4;hTAU-GFP/*sgg*^[M11] or APPL-GAL4;hTAU-GFP/*psn*^[12] larvae, females that were APPL-GAL4;SGG^{WT}/B3, APPL-GAL4;*sgg*^[M11]/B3, or APPL-GAL4;*psn*^[12]/B3 were generated and crossed to hTAU-GFP males and non-tubby female larvae from this cross was used for *in vivo* analysis. Third instar larvae were dissected on a sylgard platform using Ca²⁺-free buffer containing the following, NaCl (128 mM), EGTA (1 mM), MgCl₂ (4 mM), KCl (2 mM), HEPES (5 mM) and sucrose (36 mM) as described in Kuznicki *et al.* (48). Dissected animals were inverted onto a cover slip and imaged using a Nikon Eclipse TE 2000-U inverted microscope with a Coolsnap HQ camera and a 100 ×/1.40NA oil objective. One hundred and fifty frames of videos were collected at 200 ms exposure under the control of Metamorph software. For each genotype, four time-lapsed movies were collected for each animal; five animals were imaged; a total of 20 movies were collected.

In vivo movement analysis

In vivo movement analysis was performed as described in Reis *et al.* (69) and Gunawardena *et al.* (12). Briefly, GFP-tagged vesicles/organelles in time-lapse movies were detected as single particles as described in Yang *et al.* (70). Their full trajectories were recovered using customized software based on the modification of the single particle tracking technique described in Ponti *et al.* (71). Since the particle tracking output contained mainly trajectory segments, a further computational process was performed to link these segments into full trajectories. Finally, a manual process was used to recover trajectories that the software was unable to recover. All recovered trajectories were manually inspected so that errors were either corrected or removed. For each genotype, individual cargoes were automatically classified as being either stationary, anterograde, retrograde or reversing. Cargo trajectories of each genotype were then analyzed by calculating different descriptors that

characterize the overall distribution of cargo population and individual cargo behavior in terms of velocity, pause, run lengths and reversals (switches) (12,69). In particular, to determine the velocity of a specific cargo, its trajectory is first partitioned into segments that are uninterrupted by pause or reversal events. For a given direction, either anterograde or retrograde, duration-weighted segmental velocity of the cargo is defined by its total distance of movement divided by its total duration of movement in that direction. This definition effectively weights cargo velocities within different segments by their durations. All data analysis was conducted using customized software written in MATLAB (Mathworks) and C++ and in-depth details are provided in (12,69).

Statistics

For immunofluorescence analysis of axonal blockages, statistical analysis was performed using Excel (Microsoft Corp.), using the two-sample two-sided Student's *t*-test, and two other multiple comparison procedures (the Bonferroni and Dunnett procedures) specifically designed to compare each treatment with a control. Differences were considered significant at a significance level of 0.05, which means a 95% statistically significant correlation. All three statistical methods revealed similar significant differences. For *in vivo* movement analysis, as previously done, data were first checked for normality using three different tests implemented in the *nortest* package of R: the Lilliefors test, the Anderson-Darling test and the Shapiro-Francis test (12,69). For those that generally follow normal distributions, their means were compared using the two-sample two-sided Student's *t*-test. For those following non-normal distributions, their means were compared using the permutation *T*-test (72) or the Wilcoxon rank-sum test.

Membrane floatation and western blot analysis:

As previously described, 5 mls of larval brains from each genotype (psn^[12]−/+ , SGG^{ACTIVE} or sgg^[M11]−/+) were homogenized in acetate buffer (10 mM HEPES, pH 7.4, 100 mM K acetate, 150 mM sucrose, 5 mM EGTA, 3 mM Mg acetate, 1 mM DTT) with proteinase and phosphatase inhibitors (25). Debris was removed by centrifugation at 1000g for 7 min, and the resulting PNS was brought to 40% sucrose, bottom loaded and overlaid with two cushions of 35 and 8% sucrose. The gradient was centrifuged at 50 000 rpm in a TLS55 rotor (Beckman Coulter, Fullerton, CA, USA) for 1 h. Light membranous organelles and membrane-associated proteins floated to the 35/8 interface, whereas heavier membranes and mitochondria were found in the pellet. Equal amounts of protein from the PNS, 35/8 interface, soluble and pellet fractions were analyzed by western blotting. Antibodies pSer9 GSK-3b monoclonal antibody (Abcam at 1:500), pY216 GSK-3b monoclonal antibody (Abcam at 1:500), GSK-3b total monoclonal antibody (Abcam at 1:100), anti-KHC polyclonal antibody (Cytoskeleton at 1:1000), anti-DIC74kd monoclonal antibody (Millipore at 1:100), anti-tubulin monoclonal antibody (Abcam at 1:1000 dilution) and anti-actin monoclonal antibody (Abcam at 1:1000 dilution) were used. Immunoreaction was detected using the ECL kit (Pharmacia) and imaged using QuantityOne (Bio-Rad). Quantification analysis was performed using NIH ImageJ

software. Each lane of the gel was analyzed using plot lane, wand and label peaks gel analysis functions. Data obtained as percent values for each sample by Image J were analyzed in Excel (Microsoft Corp.). Relative intensity was calculated by dividing the percent value for each sample by percent value of syntaxin and then normalized to WT, so that WT was 1. Using the two-sample two-sided Student's *t*-test, differences were considered significant at a significance level of 0.05, which means a 95% statistically significant correlation from three separate membranes from three different experiments.

SUPPLEMENTARY MATERIAL

Supplementary Material is available at *HMG* online.

ACKNOWLEDGEMENTS

We thank Tymish Ohulchanskyy for assistance with the Leica Confocal microscope, Stefan Roberts for assistance with biochemical assays, Ge Yang and Minhua Qiu for assistance with *in vivo* data analysis, Margaret Hollingsworth for critical reading of the manuscript, Priyantha Karunaratne for constant support and members of the Gunawardena laboratory for constructive discussions.

FUNDING

This work was supported by funds from the John R. Oishei Foundation to SG and a Fulbright Scholarship (Tibetan Fund) to K.D. G.J.I., K.H.Z. and E.S. were supported by fellowships from the University at Buffalo (UB) Center for Undergraduate Research and Creative Activities (CURCA).

REFERENCES

- Woodgett, J.R. (1990) Molecular cloning and expression of glycogen synthase kinase-3/factor A. *EMBO J.*, **9**, 2431–2438.
- Woodgett, J.R. (1991) cDNA cloning and properties of glycogen synthase kinase-3. *Methods Enzymol.*, **200**, 564–577.
- Hur, E.M. and Zhou, F.Q. (2010) GSK3 signalling in neural development. *Nat. Rev. Neurosci.*, **11**, 539–551.
- Hughes, K., Nikolakaki, E., Plyte, S.E., Totty, N.F. and Woodgett, J.R. (1993) Modulation of the glycogen synthase kinase-3 family by tyrosine phosphorylation. *EMBO J.*, **12**, 803–808.
- Plyte, S.E., Hughes, K., Nikolakaki, E., Pulverer, B.J. and Woodgett, J.R. (1992) Glycogen synthase kinase-3: functions in oncogenesis and development. *Biochim. Biophys. Acta*, **1114**, 147–162.
- Wang, Q.M., Fiol, C.J., DePaoli-Roach, A.A. and Roach, P.J. (1994) Glycogen synthase kinase-3beta is a dual specificity kinase differentially regulated by tyrosine and serine/threonine phosphorylation. *J. Biol. Chem.*, **269**, 14566–14574.
- Grimes, C.A. and Jope, R.S. (2001) The multifaceted roles of glycogen synthase kinase 3beta in cellular signaling. *Prog. Neurobiol.*, **65**, 391–426.
- Gantier, R., Gilbert, D., Dumanchin, C., Campion, D., Davoust, D., Toma, F. and Frebourg, T. (2000) The pathogenic L392V mutation of presenilin 1 decreases the affinity to glycogen synthase kinase-3beta. *Neurosci. Lett.*, **283**, 217–220.
- Takashima, A., Murayama, M., Murayama, O., Kohno, T., Honda, T., Yasutake, K., Nihonmatsu, N., Mercken, M., Yamaguchi, H., Sugihara, S. and Wolozin, B. (1998) Presenilin 1 associates with glycogen synthase kinase-3beta and its substrate tau. *Proc. Natl Acad. Sci. USA*, **95**, 9637–9641.
- Kang, D.E., Soriano, S., Frosch, M.P., Collins, T., Naruse, S., Sisodia, S.S., Leibowitz, G., Levine, F. and Koo, E.H. (1999) Presenilin 1 facilitates the

- constitutive turnover of beta-catenin: differential activity of Alzheimer's disease-linked PS1 mutants in the beta-catenin-signaling pathway. *J. Neurosci.*, **19**, 4229–4237.
11. Weaver, C., Leidel, C., Szpankowski, L., Farley, N.M., Shubeita, G.T. and Goldstein, L.S. (2013) Endogenous GSK-3/Shaggy Regulates Bidirectional axonal transport of the amyloid precursor protein. *Traffic*, **14**, 295–308.
 12. Gunawardena, S., Yang, G. and Goldstein, L.S. (2013) Presenilin controls kinesin-1 and dynein function during APP vesicle transport *in vivo*. *Hum. Mol. Genet.*, **22**, 3828–3843.
 13. Pigino, G., Morfini, G., Pelsman, A., Mattson, M.P., Brady, S.T. and Busciglio, J. (2003) Alzheimer's presenilin 1 mutations impair kinesin-based axonal transport. *J. Neurosci.*, **23**, 4499–4508.
 14. Lazarov, O., Morfini, G.A., Pigino, G., Gadadhar, A., Chen, X., Robinson, J., Ho, H., Brady, S.T. and Sisodia, S.S. (2007) Impairments in fast axonal transport and motor neuron deficits in transgenic mice expressing familial Alzheimer's disease-linked mutant presenilin 1. *J. Neurosci.*, **27**, 7011–7020.
 15. Lee, K.D. and Hollenbeck, P.J. (1995) Phosphorylation of kinesin *in vivo* correlates with organelle association and neurite outgrowth. *J. Biol. Chem.*, **270**, 5600–5605.
 16. Morfini, G., Szebenyi, G., Elluru, R., Ratner, N. and Brady, S.T. (2002) Glycogen synthase kinase-3 phosphorylates kinesin light chains and negatively regulates kinesin-based motility. *EMBO J.*, **21**, 281–293.
 17. Ali, A., Hoefflich, K.P. and Woodgett, J.R. (2001) Glycogen synthase kinase-3: properties, functions, and regulation. *Chem. Rev.*, **101**, 2527–2540.
 18. Mudher, A., Shepherd, D., Newman, T.A., Mildren, P., Jukes, J.P., Squire, A., Mears, A., Drummond, J.A., Berg, S., MacKay, D., Asuni, A.A., Bhat, R. and Lovestone, S. (2004) GSK-3beta inhibition reverses axonal transport defects and behavioural phenotypes in *Drosophila*. *Mol. Psychiatry*, **9**, 522–530.
 19. Dixit, R., Ross, J.L., Goldman, Y.E. and Holzbaur, E.L. (2008) Differential regulation of dynein and kinesin motor proteins by tau. *Science*, **319**, 1086–1089.
 20. Cuchillo-Ibanez, I., Seeceram, A., Byers, H.L., Leung, K.Y., Ward, M.A., Anderton, B.H. and Hanger, D.P. (2008) Phosphorylation of tau regulates its axonal transport by controlling its binding to kinesin. *FASEB J.*, **22**, 3186–3195.
 21. Falzone, T.L., Stokin, G.B., Lillo, C., Rodrigues, E.M., Westerman, E.L., Williams, D.S. and Goldstein, L.S. (2009) Axonal stress kinase activation and tau misbehavior induced by kinesin-1 transport defects. *J. Neurosci.*, **29**, 5758–5767.
 22. Hurd, D.D. and Saxton, W.M. (1996) Kinesin mutations cause motor neuron disease phenotypes by disrupting fast axonal transport in *Drosophila*. *Genetics*, **144**, 1075–1085.
 23. Bowman, A.B., Patel-King, R.S., Benashski, S.E., McCaffery, J.M., Goldstein, L.S. and King, S.M. (1999) *Drosophila* roadblock and Chlamydomonas LC7: a conserved family of dynein-associated proteins involved in axonal transport, flagellar motility, and mitosis. *J. Cell Biol.*, **146**, 165–180.
 24. Gindhart, J.G., Desai, C.J., Beushausen, S., Zinn, K. and Goldstein, L.S. (1998) Kinesin light chains are essential for axonal transport in *Drosophila*. *J. Cell Biol.*, **141**, 443–454.
 25. Haghnia, M., Cavalli, V., Shah, S.B., Schimmelpfeng, K., Brusch, R., Yang, G., Herrera, C., Pilling, A. and Goldstein, L.S. (2007) Dynactin is required for coordinated bidirectional motility, but not for dynein membrane attachment. *Mol. Biol. Cell*, **18**, 2081–2089.
 26. Horiuchi, D., Collins, C.A., Bhat, P., Barkus, R.V., Diantonio, A. and Saxton, W.M. (2007) Control of a kinesin-cargo linkage mechanism by JNK pathway kinases. *Curr. Biol.*, **17**, 1313–1317.
 27. Gunawardena, S. and Goldstein, L.S. (2001) Disruption of axonal transport and neuronal viability by amyloid precursor protein mutations in *Drosophila*. *Neuron*, **32**, 389–401.
 28. Falzone, T.L., Gunawardena, S., McCleary, D., Reis, G.F. and Goldstein, L.S. (2010) Kinesin-1 transport reductions enhance human tau hyperphosphorylation, aggregation and neurodegeneration in animal models of tauopathies. *Hum. Mol. Genet.*, **19**, 4399–4408.
 29. Gunawardena, S., Her, L.S., Brusch, R.G., Laymon, R.A., Niesman, I.R., Gordesky-Gold, B., Sintasath, L., Bonini, N.M. and Goldstein, L.S. (2003) Disruption of axonal transport by loss of huntingtin or expression of pathogenic polyQ proteins in *Drosophila*. *Neuron*, **40**, 25–40.
 30. Power, D., Srinivasan, S. and Gunawardena, S. (2012) In-vivo evidence for the disruption of Rab11 vesicle transport by loss of huntingtin. *Neuroreport*, **23**, 970–977.
 31. Bowman, A.B., Kamal, A., Ritchings, B.W., Philp, A.V., McGrail, M., Gindhart, J.G. and Goldstein, L.S. (2000) Kinesin-dependent axonal transport is mediated by the Sunday driver (SYD) protein. *Cell*, **103**, 583–594.
 32. Perrimon, N. and Smouse, D. (1989) Multiple functions of a *Drosophila* homeotic gene, zeste-white 3, during segmentation and neurogenesis. *Dev. Biol.*, **135**, 287–305.
 33. Hong, C.S. and Koo, E.H. (1997) Isolation and characterization of *Drosophila* presenilin homolog. *Neuroreport*, **8**, 665–668.
 34. Boulianne, G.L., Livne-Bar, I., Humphreys, J.M., Liang, Y., Lin, C., Rogaev, E. and St George-Hyslop, P. (1997) Cloning and characterization of the *Drosophila* presenilin homologue. *Neuroreport*, **8**, 1025–1029.
 35. Ye, Y. and Fortini, M.E. (1998) Characterization of *Drosophila* presenilin and its colocalization with Notch during development. *Mech. Dev.*, **79**, 199–211.
 36. Struhl, G. and Greenwald, I. (1999) Presenilin is required for activity and nuclear access of Notch in *Drosophila*. *Nature*, **398**, 522–525.
 37. Ye, Y., Lukinova, N. and Fortini, M.E. (1999) Neurogenic phenotypes and altered Notch processing in *Drosophila* presenilin mutants. *Nature*, **398**, 525–529.
 38. Lukinova, N.I., Roussakova, V.V. and Fortini, M.E. (1999) Genetic characterization of cytological region 77A-D harboring the presenilin gene of *Drosophila melanogaster*. *Genetics*, **153**, 1789–1797.
 39. Nuydens, R., Van Den Kieboom, G., Nolten, C., Verhulst, C., Van Osta, P., Spittaels, K., Van den Haute, C., De Feyter, E., Geerts, H. and Van Leuven, F. (2002) Coexpression of GSK-3beta corrects phenotypic aberrations of dorsal root ganglion cells, cultured from adult transgenic mice overexpressing human protein tau. *Neurobiol. Dis.*, **9**, 38–48.
 40. Stamer, K., Vogel, R., Thies, E., Mandelkow, E. and Mandelkow, E.M. (2002) Tau blocks traffic of organelles, neurofilaments, and APP vesicles in neurons and enhances oxidative stress. *J. Cell Biol.*, **156**, 1051–1063.
 41. Brownlee, J., Irving, N.G., Brion, J.P., Gibb, B.J., Wagner, U., Woodgett, J. and Miller, C.C. (1997) Tau phosphorylation in transgenic mice expressing glycogen synthase kinase-3beta transgenes. *Neuroreport*, **8**, 3251–3255.
 42. Ebner, A., Godemann, R., Stamer, K., Illenberger, S., Trinczek, B. and Mandelkow, E. (1998) Overexpression of tau protein inhibits kinesin-dependent trafficking of vesicles, mitochondria, and endoplasmic reticulum: implications for Alzheimer's disease. *J. Cell Biol.*, **143**, 777–794.
 43. Jancsik, V., Filliol, D. and Rendon, A. (1996) Tau proteins bind to kinesin and modulate its activation by microtubules. *Neurobiology*, **4**, 417–429.
 44. Trinczek, B., Ebner, A., Mandelkow, E.M. and Mandelkow, E. (1999) Tau regulates the attachment/detachment but not the speed of motors in microtubule-dependent transport of single vesicles and organelles. *J. Cell Sci.*, **112**, 2355–2367.
 45. LaPointe, N.E., Morfini, G., Pigino, G., Gaisina, I.N., Kozikowski, A.P., Binder, L.I. and Brady, S.T. (2009) The amino terminus of tau inhibits kinesin-dependent axonal transport: implications for filament toxicity. *J. Neurosci. Res.*, **87**, 440–451.
 46. Xiong, X. and Collins, C.A. (2012) A conditioning lesion protects axons from degeneration via the Wallenda/DLK MAP kinase signaling cascade. *J. Neurosci.*, **32**, 610–615.
 47. Estes, P.S., Ho, G.L., Narayanan, R. and Ramaswami, M. (2000) Synaptic localization and restricted diffusion of a *Drosophila* neuronal synaptobrevin—green fluorescent protein chimera *in vivo*. *J. Neurogenet.*, **13**, 233–255.
 48. Kuznicki, M.L. and Gunawardena, S. (2010) In vivo visualization of synaptic vesicles within *Drosophila* larval segmental axons. *J. Vis. Exp.*, **44**, 2151.
 49. Papp, H., Pakaski, M. and Kasa, P. (2002) Presenilin-1 and the amyloid precursor protein are transported bidirectionally in the sciatic nerve of adult rat. *Neurochem. Int.*, **41**, 429–435.
 50. Kasa, P., Papp, H. and Pakaski, M. (2001) Presenilin-1 and its N-terminal and C-terminal fragments are transported in the sciatic nerve of rat. *Brain Res.*, **909**, 159–169.
 51. Sheng, J.G., Price, D.L. and Koliatsos, V.E. (2003) The beta-amyloid-related proteins presenilin 1 and BACE1 are axonally transported to nerve terminals in the brain. *Exp. Neurol.*, **184**, 1053–1057.
 52. Kamal, A., Almenar-Queralt, A., LeBlanc, J.F., Roberts, E.A. and Goldstein, L.S.B. (2001) Kinesin-mediated axonal transport of a membrane

- compartment containing beta-secretase and presenilin-1 requires APP. *Nature*, **414**, 643–648.
53. Hollenbeck, P.J. (1993) Phosphorylation of neuronal kinesin heavy and light chains *in vivo*. *J Neurochem*, **60**, 2265–2275.
 54. McDonald, A., Fogarty, S., Leclerc, I., Hill, E.V., Hardie, D.G. and Rutter, G.A. (2012) Cell-wide analysis of secretory granule dynamics in three dimensions in living pancreatic beta-cells: evidence against a role for AMPK-dependent phosphorylation of KLC1 at Ser517/Ser520 in glucose-stimulated insulin granule movement. *Biochem. Soc. Trans.*, **38**, 205–208.
 55. Schäfer, B., Götz, C., Dudek, J., Hessenauer, A., Matti, U. and Montenarh, M. (2009) KIF5C: a new binding partner for protein kinase CK2 with a preference for the CK2alpha' subunit. *Cell Mol. Life Sci.*, **66**, 339–349.
 56. Verhey, K.J., Lizotte, D.L., Abramson, T., Barenboim, L., Schnapp, B.J. and Rapoport, T.A. (1998) Light chain-dependent regulation of Kinesin's interaction with microtubules. *J. Cell Biol.*, **143**, 1053–1066.
 57. Kennelly, P.J. and Krebs, E.G. (1991) Consensus sequences as substrate specificity determinants for protein kinases and protein phosphatases. *J. Biol. Chem.*, **266**, 15555–15558.
 58. Whyte, J., Bader, J.R., Tauhata, S.B., Raycroft, M., Hornick, J., Pfister, K.K., Lane, W.S., Chan, G.K., Hinchcliffe, E.H., Vaughan, P.S. and Vaughan, K.T. (2008) Phosphorylation regulates targeting of cytoplasmic dynein to kinetochores during mitosis. *J. Cell Biol.*, **183**, 819–834.
 59. Song, Y., Benison, G., Nyarko, A., Hays, T.S. and Barbar, E. (2007) Potential role for phosphorylation in differential regulation of the assembly of dynein light chains. *J. Biol. Chem.*, **282**, 17272–17279.
 60. Dillman, J.F. 3rd. and Pfister, K.K. (1994) Differential phosphorylation *in vivo* of cytoplasmic dynein associated with anterogradely moving organelles. *J. Cell Biol.*, **127**, 1671–1681.
 61. Kirschenbaum, F., Hsu, S.C., Cordell, B. and McCarthy, J.V. (2001) Substitution of a glycogen synthase kinase-3beta phosphorylation site in presenilin 1 separates presenilin function from beta-catenin signalling. *J. Biol. Chem.*, **276**, 7366–7375.
 62. Kirschenbaum, F., Hsu, S.C., Cordell, B. and McCarthy, J.V. (2001) Glycogen synthase kinase-3beta regulates presenilin 1 C-terminal fragment levels. *J. Biol. Chem.*, **276**, 30701–30707.
 63. Tesco, G. and Tanzi, R.E. (2000) GSK3 beta forms a tetrameric complex with endogenous PS1-CTF/NTF and beta-catenin. Effects of the D257/D385A and FAD-linked mutations. *Ann. N Y Acad. Sci.*, **920**, 227–232.
 64. Blasius, T.L., Cai, D., Jih, G.T., Toret, C.P. and Verhey, K.J. (2007) Two binding partners cooperate to activate the molecular motor kinesin-1. *J. Cell Biol.*, **176**, 11–17.
 65. Hanger, D.P., Hughes, K., Woodgett, J.R., Brion, J.P. and Anderton, B.H. (1992) Glycogen synthase kinase-3 induces Alzheimer's disease-like phosphorylation of tau: generation of paired helical filament epitopes and neuronal localisation of the kinase. *Neurosci. Lett.*, **147**, 58–62.
 66. Phiel, C.J., Wilson, C.A., Lee, V.M. and Klein, P.S. (2003) GSK-3alpha regulates production of Alzheimer's disease amyloid-beta peptides. *Nature*, **423**, 435–439.
 67. Bourouis, M. (2002) Targeted increase in shaggy activity levels blocks wingless signaling. *Genesis*, **34**, 99–102.
 68. Fye, S., Dolma, K., Kang, M.J. and Gunawardena, S. (2010) Visualization of larval segmental nerves in 3rd instar *Drosophila* larval preparations. *J. Vis. Exp.*, **43**, pii: 2128. doi: 10.3791/2128.
 69. Reis, G.F., Yang, G., Szpankowski, L., Shah, S.B., Robinson, J.T., Hays, T.S., Danuser, G. and Goldstein, L.S.B. (2012) Molecular motor function in axonal transport *in vivo* probed by genetic and computational analysis in *Drosophila*. *Mol. Biol. Cell*, **23**, 1700–1714.
 70. Yang, G., Matov, A. and Danuser, G. (2005) Reliable tracking of large-scale dense particle motion for fluorescent live cell imaging. *Proc. IEEE Int Conf Comput Vis Pattern Recognit*, **3**, 138.
 71. Ponti, A., Vallotton, P., Salmon, W.C., Waterman-Storer, C.M. and Danuser, G. (2003) Computational analysis of F-actin turnover in cortical actin meshworks using fluorescent speckle microscopy. *Biophys. J.*, **84**, 3336–3352.
 72. Moore, D.S. and McCabe, G.P. (2005) *Introduction to the practice of statistics*, 5th edn. W.H. Freeman, New York.